

SP8T Switch Design using Cascaded SPDT Switches for Monostatic Microwave Imaging System in Medical Application

Abstract. This paper proposes a single pole eight throw switch (SP8T) using cascaded single pole double throw (SPDT) switches. The switch design is to control eight antenna array in the monostatic microwave imaging system for medical application. A mathematical modeling was done for a simple series-shunt SPDT switch for the analysis of insertion loss, return loss and isolation. Then, a proper selection of SPDT switch topologies was carried out in a simulation software in order to get ultra wideband (UWB) performance of the SP8T switch design. As a result, the proposed SP8T switch produced 9.3 GHz of isolation bandwidth that can be used for a Gaussian pulse up to 9.3 GHz bandwidth (from 1.7 GHz to 11 GHz frequency spectrum).

Streszczenie. W niniejszym artykule zaproponowano jednobiegunowy przełącznik ośmiururowy (SP8T) wykorzystujący kaskadowe jednobiegunowe przełączniki dwustanowe (SPDT). Konstrukcja przełącznika służy do sterowania układem ośmiu anten w monostaticznym mikrofalowym systemie obrazowania do zastosowań medycznych. Przeprowadzono modelowanie matematyczne prostego przełącznika SPDT z bocznikiem szeregowym do analizy tłumienia wtrąceniowego, tłumienia odbiciowego i izolacji. Następnie dokonano właściwego wyboru topologii przełącznika SPDT w oprogramowaniu symulacyjnym, aby uzyskać wydajność ultraszerokopasmową (UWB) projektu przełącznika SP8T. W rezultacie proponowany przełącznik SP8T wytworzył pasmo izolacji 9,3 GHz, które można wykorzystać dla impulsu Gaussa o szerokości do 9,3 GHz (widmo częstotliwości od 1,7 GHz do 11 GHz). (Konstrukcja przełącznika SP8T z wykorzystaniem kaskadowych przełączników SPDT do monostaticznego systemu obrazowania mikrofalowego w zastosowaniach medycznych)

Keywords: PIN diode switch, SP8T, SPDT, ultra wideband, UWB, microwave imaging.

Słowa kluczowe: obrazowanie mikrofalowe, przełączniki sp8T, WWB

Introduction

In designing a microwave imaging system for medical application, it can use a monostatic radar approach by transmitting a Gaussian pulse (with an ultra wideband (UWB) frequency) through antennas [1, 2]. As depicted in Fig. 1, any microwave system using one antenna acts as both transmitter and receiver and the signal is analyzed by interrogating the reflecting signal [3, 4]. The antenna is an ultra wideband performance as reported in [5, 6] and a confocal algorithm is used to shape an image based on the captured reflected signal.

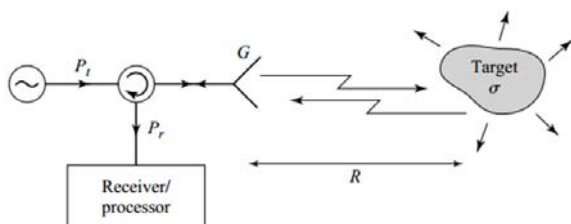


Fig. 1. Concept of monostatic radar in a microwave system [3]

Antenna array is normally used with half wavelength element-to-element spacing to estimate the real-time imagery of targets [7]. A minimum of eight antennas can be used in microwave imaging systems [8, 9, 10].

It is found that, Radio Frequency (RF) switches are commonly used for microwave imaging to support and control multiple antennas for transmit and receive signals. As depicted in Fig. 2, it is an example of RF switch used in breast imaging system for antenna array switching [11]. The RF switch must be an UWB performance for the insertion loss, return loss and also isolation.

However, due the unsuitable of RF switch design (e.g. wrong selection of switch topology), there will be RF leakages to another unused antenna, thus deteriorate the microwave imaging system performance. Hence, for the best RF switch design, it should be able to reduce a

leakage signal from off-path port during transmit or receive mode [12, 13]. Therefore, a proper design of RF switch is important to ensure the power of signals from the pulse generator is reaching to the antenna with minimum losses [14, 9] and a good isolation performance is needed to remove any leakage signal due to multiple antenna configurations in microwave imaging systems [15, 16].

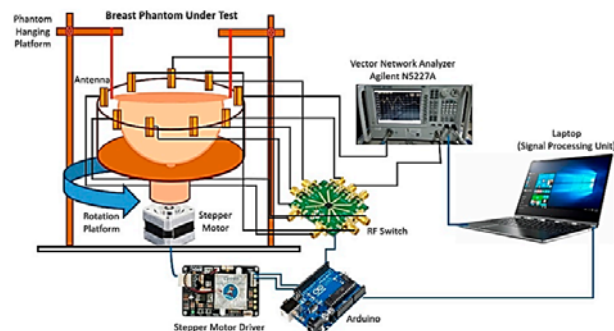


Fig. 2. RF switch in breast imaging system for antenna array switching [11]

Therefore, this paper proposes a single pole eight throw (SP8T) switch for monostatic microwave imaging system in medical application. It was designed in the frequency range from 1 to 11 GHz. The switch design is to control eight antenna array in the system. The proposed SP8T switch is based on a cascaded single pole double throw (SPDT). With the proper selection of switch topology and switching element (e.g. PIN diode), UWB isolation performance of the RF switch can be achieved but need to look at the other trade off as well such as return loss or insertion loss performances.

SP8T Switch Design

The proposed SP8T switch is shown in Fig. 3. In this figure, Port 1 is an input for transmit and receive of

Gaussian pulse signal, while Port 2 until 9 are connected to 8 antenna arrays. A cascaded of seven SPDT switches is the key element in the SP8T switch, due its capability to get high isolation performance by selecting a suitable SPDT switch topology.

Besides that, MACOM's PIN diodes (MA4SPS402) were used in the SP8T switch as the switching elements. The PIN diodes were made from silicon glass. By referring to the product datasheet, these PIN diodes are suitable for high frequency applications which have a maximum frequency of 18 GHz. Hence, the selection of the PIN diode contributed also to the performance of the SP8T switch design.

The performance analysis of SP8T switch is based on the insertion loss, return loss and isolation. Take an example operation during transmission of Gaussian pulse signal that inserted into Port 1 and transmitted to antenna No. 2 at Port 2. The insertion loss is simulated or measured between Port 1 and Port 2 (S_{21}) meanwhile the return loss is at Port 1 (S_{11}). For the isolation, it can be simulated at any unused antennas (No 3 until No 9). In this paper the isolation was simulated and measured at antenna No. 3, between Port 1 and 3 (S_{31}).

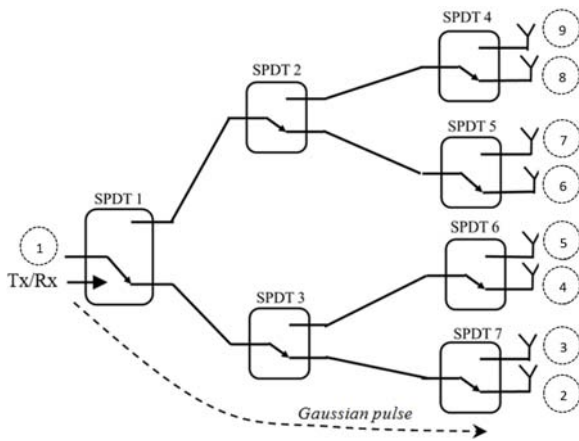


Fig. 3. Cascaded SPDT switches in UWB SP8T switch

Selection of SPDT Switch Topology

The performance analysis of SPDT circuit is important to find the best topologies to be further developed in SPDT for the SP8T switch circuit. As reported in [17], designing a wideband and broadband RF switches are more challenging compared to narrowband RF switches. It requires very wideband or broadband of isolation, insertion loss and return loss. Broadband or wideband isolation can be achieved by combining several techniques such as RF switch topology and combined with the use of fabrication process of PIN diode or transistor. In our previous research work of RF switch for wireless communication [18], the series-shunt-shunt is the best topology for broadband isolation. Furthermore, the series-shunt PIN diode is the most chosen topology in order to get an ultra wideband isolation performance [19, 20, 21, 22, 23].

A mathematical modeling can be done for a simple series-shunt SPDT switch (Design A) as shown in Fig. 4. A basic series-shunt is selected for the mathematical analysis of the insertion loss, return loss and isolation. Considering a transmission of the Gaussian pulse from Port 1 to Port 2. Then, the insertion loss can be analyzed as S_{21} , the return loss as S_{11} and isolation as S_{31} .

Table 1 is a circuit operation of Design A during a transmission of Gaussian pulse from Port 1 to Port 2. In this operation, the series PIN diode of D1b was turned ON and series PIN diode of D1a was turned OFF with the voltage supplies of $VCC\ 1 = +5\ V$ and $VCC\ 2 = -5\ V$. Meanwhile, shunt PIN diodes of D2b were in OFF state to ensure there

is no RF leakage from Port 1 to Port 2 and shunt PIN diodes of D2a was in ON state to isolate any RF signal from entering to Port 3.

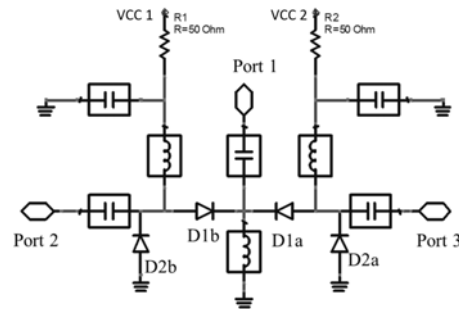


Fig. 4. Series-shunt SPDT topology (Design A)

Table 1: Circuit operation of series-shunt SPDT switch

Label	Value/Condition
VCC 1	+ 5 V
VCC 2	- 5 V
D1a (series)	OFF state (reverse bias)
D2a (shunt)	ON state (forward bias)
D1b (series)	ON state (forward bias)
D2b (shunt)	OFF state (reverse bias)

In the mathematical analysis of the insertion loss (S_{21}) and return loss (S_{11}), the ABCD matrix of series-shunt SPDT for transmission of the Gaussian pulse from Port 1 to Port 2 is given by,

$$(1) \quad [T_{12}] = [T_{D1b}][T_{D2b}]$$

$$= \begin{bmatrix} 1 & R_f + j\omega L_s \\ 0 & 1 \end{bmatrix} \begin{bmatrix} 1 & 0 \\ \frac{1}{R_r + j\omega L_s + \frac{1}{j\omega C_j}} & 1 \end{bmatrix}$$

$$= \begin{bmatrix} \left(\frac{R_f + j\omega L_s}{R_r + j\omega L_s + \frac{1}{j\omega C_j}} + 1 \right) (R_f + j\omega L_s) & \\ \left(\frac{1}{R_r + j\omega L_s + \frac{1}{j\omega C_j}} \right) & 1 \end{bmatrix}$$

where R_f is forward bias resistance, L_s is series inductance, R_r is reverse bias resistance and C_j is junction capacitance in the PIN diode [3].

For the insertion loss, the ABCD matrix of (1) is converted to S-parameter of S_{21} . Thus,

$$(2) \quad S_{21} = \frac{2}{A + \frac{B}{Z_0} + CZ_0 + D}$$

$$= \frac{2}{2 + \frac{R_f + j\omega L_s}{Z_0} + \frac{Z_0}{R_r + j\omega L_s + \frac{1}{j\omega C_j}} + \frac{R_f + j\omega L_s}{R_r + j\omega L_s + \frac{1}{j\omega C_j}}}$$

By referring to (2), very low insertion loss can be obtained if the PIN diode impedance during ON state is close to zero and the PIN diode impedance during OFF state is very high. In this case, the characteristic impedance Z_0 is normalized to 1.

For the return loss, the ABCD matrix of (1) is converted to S-parameter of S_{11} . Thus,

$$S_{11} = \frac{A + \frac{B}{Z_0} - CZ_0 - D}{A + \frac{B}{Z_0} + CZ_0 + D} \quad (3)$$

$$= \frac{\left(\frac{R_f + j\omega L_s}{R_f + j\omega L_s + \frac{1}{j\omega C_j}} + \frac{R_f + j\omega L_s}{Z_0} - \frac{Z_0}{R_f + j\omega L_s + \frac{1}{j\omega C_j}} \right)}{\left(2 + \frac{R_f + j\omega L_s}{Z_0} + \frac{Z_0}{R_f + j\omega L_s + \frac{1}{j\omega C_j}} + \frac{R_f + j\omega L_s}{R_f + j\omega L_s + \frac{1}{j\omega C_j}} \right)}$$

It can be seen in (3) where a very high return loss can be obtained if the PIN diode impedance during ON state is close to zero and the PIN diode impedance during OFF state is very high. In this case, the characteristic impedance Z_0 is normalized to 1.

In the mathematical analysis for the isolation (S_{31}), the ABCD matrix of series-shunt SPDT for isolation of the Gaussian pulse from Port 1 to Port 3 is given by,

$$[T_{13}] = [T_{D1a}][T_{D2a}] \quad (4)$$

$$= \begin{bmatrix} 1 & R_f + j\omega L_s + \frac{1}{j\omega C_j} \\ 0 & 1 \end{bmatrix} \begin{bmatrix} 1 & 0 \\ \frac{1}{R_f + j\omega L_s} & 1 \end{bmatrix}$$

$$= \begin{bmatrix} \left(R_f + j\omega L_s + \frac{1}{j\omega C_j} \right) & \\ 1 + \frac{R_f + j\omega L_s + \frac{1}{j\omega C_j}}{R_f + j\omega L_s} & \left(R_f + j\omega L_s + \frac{1}{j\omega C_j} \right) \\ \left(\frac{1}{R_f + j\omega L_s} \right) & 1 \end{bmatrix}$$

The ABCD matrix of (4) is then converted to S-parameter of S_{31} . Thus,

$$S_{31} = \frac{2}{A + \frac{B}{Z_0} + CZ_0 + D} \quad (5)$$

$$= \frac{2}{2 + \frac{R_f + j\omega L_s + \frac{1}{j\omega C_j}}{R_f + j\omega L_s} + \frac{R_f + j\omega L_s + \frac{1}{j\omega C_j}}{Z_0} + \frac{Z_0}{R_f + j\omega L_s}}$$

From (5), it shows that a very high isolation can be obtained if the PIN diode impedance during ON state is close to zero and the PIN diode impedance during OFF state is very high. In this case, the characteristic impedance Z_0 is normalized to 1.

Therefore, it can be concluded that the two conditions of ON and OFF states of the PIN diodes could influence the performance of insertion loss, return loss and isolation. As reported in [24], additional shunt PIN diodes can be added in order to increase isolation. Therefore, Fig. 5 is the other three topologies (Design B, C and D) for the analysis of UWB isolation performance and the trade off with insertion loss and return loss. The analyses were done in Advanced Design System (ADS) software. All the SPDT switch topologies are summarized in Table 2 where Design A is a

series-shunt PIN diode, Design B is a series-shunt-shunt PIN diode, Design C is a series-shunt-shunt-shunt PIN diodes and Design D is a series-shunt-shunt-shunt-shunt PIN diode.

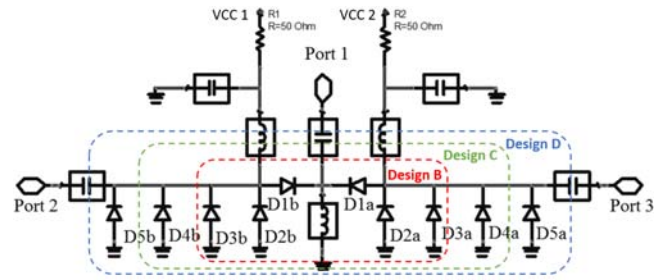


Fig. 5. Other SPDT switch topologies for Design B, C and D

Table 2: Summary of SPDT switch topologies

Design	Switch Topology	PIN diodes
Design A	series-shunt	D1a, D2a, D1b, D2b
Design B	series-shunt-shunt	D1a – D3a, D1b – D3b
Design C	series-shunt-shunt-shunt	D1a – D4a, D1b – D4b
Design D	series-shunt-shunt-shunt-shunt	D1a – D5a, D1b – D5b

Performance Analysis of Different Topologies of SPDT Switch

Fig. 6 shows a comparison of simulation results between four SPDT switch topologies. MACOM's PIN diodes (MA4SPS402) model were used in these simulations. Fig. 6(a), (b) and (c) show the performance results of return loss (S_{11}), insertion loss (S_{21}) and isolation (S_{31}) respectively. All designs simulated from 1 to 11 GHz so that it should be enough to see its capability in the UWB frequency (with 10 GHz bandwidth) for microwave medical imaging.

Overall, Design A, B, C and D produces very good S_{11} across the frequency range of 1.6 GHz to 11 GHz, as can be seen in Fig. 6(a). It was found that by adding more PIN diodes, the return loss was almost in the same response with the targeted return loss, higher than 10 dB, across the frequency range. For all designs, the lowest S_{11} was appear at 1 GHz of frequency. By contrast, Design A achieved the highest S_{11} at 10.2 GHz.

Fig. 6(b) shows that the S_{21} of Design A, B, C and D remained steady between 2 and 7 GHz at approximately 0 dB. then, it goes up at 7.5 GHz before it turns back closing to 0 dB. As can be seen, Design D showed the highest S_{21} at 7.5 GHz which still less than 1 dB. It was found that by adding more shunt PIN diodes, the S_{21} was almost in the same response with the desired result, less than 5 dB, across the simulated frequency range.

Fig. 6(c) shows that the isolations of Design A, B, C and D decreased at frequencies between 1 and 7.5 GHz before they remain steady at higher frequencies. Design D produced the highest value of isolation, about 88 dB, at 1 GHz. On the other hand, Design C produced the lowest value of isolation, about 16 dB, at 7.5 GHz. It was found that by adding more shunt PIN diodes, the isolation was improved significantly. It can be seen in average of additional 20 dB isolation improvement between Design A and D across the frequencies. Thus, for the isolation improvement, as a conclusion, there is a fact that the combination of series and shunt PIN diodes is the most chosen topology by designers.

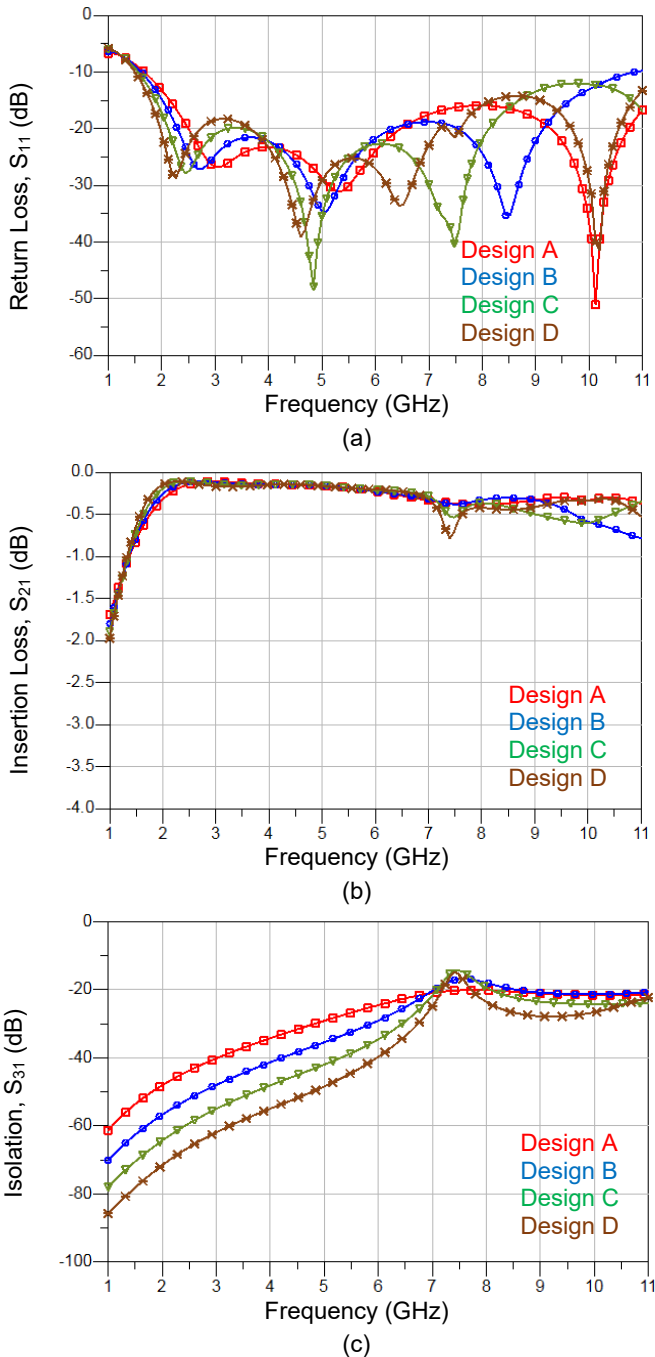


Fig. 6. Performance analysis result of SPDT; (a) return loss (S_{11}), (b) insertion loss (S_{21}), (c) isolation (S_{31})

For overall comparison, the simulation results of these four topologies showed very good outcomes in terms of return loss, insertion loss and isolation. Meanwhile, compared to other designs, Design D created very high isolation. However, Design B, also, showed a noticeable high isolation with less number of PIN diodes than Design D. Therefore, by considering the overall performances based on the minimum number of shunt PIN diodes, Design B was chosen for the cascaded SPDT in SP8T switch design due to its acceptable isolation with good insertion loss and return loss across the simulated frequency range.

Table 3 summarizes the simulation result of Design A, B, C and D. It lists the minimum (min.) and maximum (max.) results of return loss (S_{11}), insertion loss (S_{21}) and isolation (S_{31}) across the simulated frequency range (1 to 11 GHz).

Table 3. Summary of simulation result for SPDT switch topologies of Design A, B, C and D

Design	S_{11} (dB) Min & Max	S_{21} (dB) Min & Max	S_{31} (dB) Min & Max
Design A	6 & 51	0.1 & 2	20 & 61
Design B	6 & 36	0.1 & 2	18 & 70
Design C	6 & 48	0.1 & 2	16 & 79
Design D	6 & 39	0.1 & 2	17 & 88

Simulation and Measurement Results of SP8T Switch

Fig. 7 shows the fabricated SP8T switch with cascaded SPDT switches according to diagram in Fig. 3. As results, Fig. 8 shows the comparison between simulated and measured results of the SP8T switch for return loss (S_{11}), insertion loss (S_{21}) and isolation (S_{31}). These simulations and measurements were performed in the condition of the transmission of the Gaussian pulse from Port 1 to Port 2 and the isolation was at unused Antenna at Port 3. The isolation performance analysis was carried out in order to see the minimum isolation of the SP8T switch for microwave imaging system due to the single SPDT switch in the SP8T switch circuit.

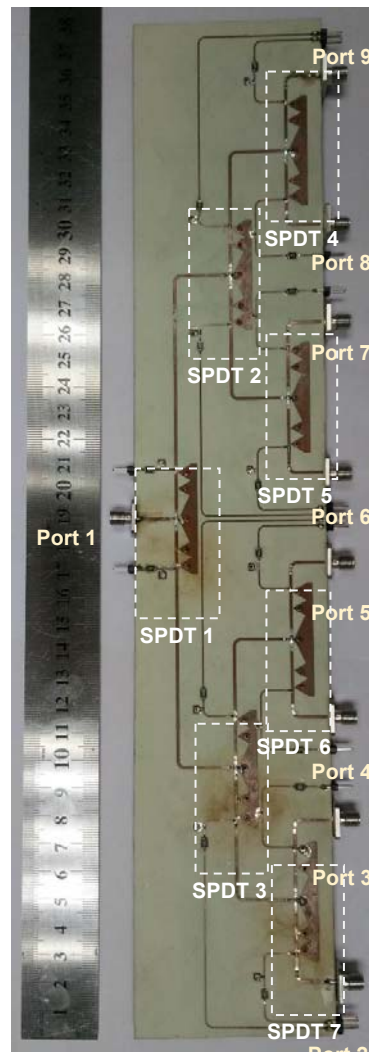


Fig. 7. Fabricated SP8T switch with cascaded SPDT switches

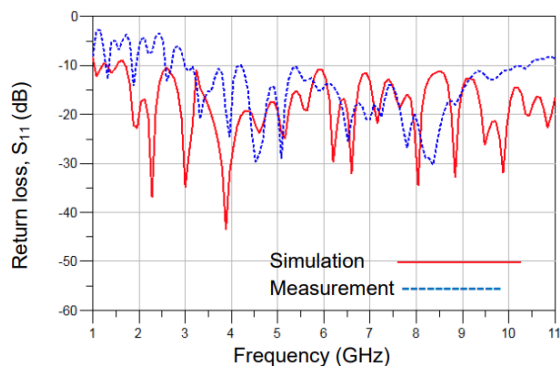
As shown in Fig. 8(a), the simulated return loss (S_{11}) showed almost a very good result from 1.7 GHz and above. The highest simulated S_{11} was around 44 dB at 3.9 GHz. Although the measured S_{11} was different compared to simulated result, but it was higher than 10 dB from 3 to 10 GHz.

As can be seen from Fig. 8(b), the simulated insertion loss (S_{21}) was neared to 0 dB from 1 to 8 GHz. Then, there was a slight increase in the simulated S_{21} in the frequencies between 8 and 9 GHz before it had been decreased in the frequencies from 9 to 10 GHz. However, the measured S_{21} was lower than 5 dB from 1 GHz to 7.5 GHz, thus the useable insertion loss bandwidth was 6.5 GHz.

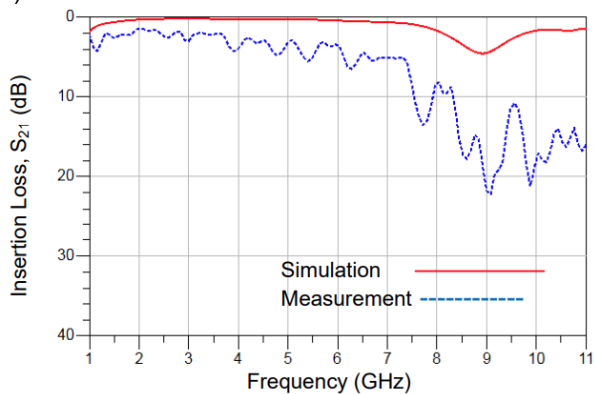
Fig. 8(c) shows the comparison between simulation and measurement results of isolation (S_{31}). Overall, the simulated and measured isolation results were very high across the operation frequency. Besides, the S_{31} in the measurement was less than in the simulation at lower frequencies (1 to 7 GHz), and vice versa at higher frequencies (8 to 11 GHz). The simulated isolation produced more than 70 dB at 1 GHz before it decreased to 20 dB at 4 GHz. Then, there was a slight increase of the S_{31} between 4 and 6 GHz, and the isolation performance remained steady from 6 to 11 GHz.

Table 4 lists the summary of simulation and measurement results of SP8T switch. This table lists the minimum (min.) and maximum (max.) results of return loss (S_{11}), insertion loss (S_{21}) and isolation (S_{31}) across the frequency range from 1 until 11 GHz.

a)



b)



c)

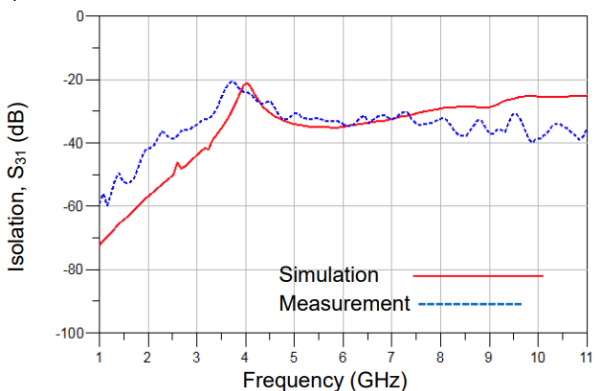


Fig. 8. Simulation versus measurement of SP8T switch; (a) return loss (S_{11}), (b) insertion loss (S_{21}) and (c) isolation (S_{31})

Table 4. Summary of simulation and measurement results of SP8T switch

	S_{11} (dB) Min & Max	S_{21} (dB) Min & Max	S_{31} (dB) Min & Max
Simulation	9 & 44	0 & 4	20 & 72
Measurement	3 & 30	2 & 22	20 & 60

Table 5 is a table for the performances of SP8T switch by referring to design specification. Generally, the proposed SP8T switch using cascaded SPDT switches produced a wide bandwidth of return loss, insertion loss and isolation. However, the usable isolation bandwidth was 9.3 GHz (sim.) and 4.5 GHz (meas.) due to low return loss at lower frequencies (1.7 GHz in simulation, 3 GHz in measurement) and higher insertion loss performance at higher frequencies (7.5 GHz in measurement). Meaning that, although the isolation bandwidth is 10 GHz (sim. and meas.), however, it was limited by the performance of return loss and insertion loss. In addition, low insertion loss in the measurement can be achieved at higher frequencies if a proper soldering of the components is carried out, thus increasing the usable isolation bandwidth in the measurement result.

Table 5. Performances of SP8T switch by referring to design specification

Performance Parameter	Specification	Bandwidth
Return Loss (S_{11})	> 10 dB	1.7 – 11 GHz (sim) BW = 9.3 GHz ----- 3 – 10.5 GHz (meas) BW = 7.5 GHz
Insertion Loss (S_{21})	< 5 dB	1 – 11 GHz (sim) BW = 10 GHz ----- 1 – 7.5 GHz (meas) BW = 6.5 GHz
Isolation (S_{31})	> 20 dB	1 – 11 GHz (sim) BW = 10 GHz ----- 1 – 11 GHz (meas) BW = 10 GHz

Conclusion

A SP8T switch using cascaded SPDT switches was designed in the frequency range from 1 to 11 GHz. The proposed SP8T switch is to control eight antenna array in the monostatic microwave imaging system for medical application. A mathematical modeling was done for a simple series-shunt SPDT switch for the analysis of insertion loss, return loss and isolation. It was found that, theoretically two conditions of ON and OFF states of the PIN diodes could influence the performance of insertion loss, return loss and isolation. Then, a proper selection of SPDT switch topologies was carried out in a simulation software in order to get ultra wideband (UWB) performance of the SP8T switch design. In the simulation analysis, by considering the overall performances based on the minimum number of shunt PIN diodes, Design B (series-shunt-shunt) was chosen for the cascaded SPDT in SP8T switch design due to its acceptable isolation with good insertion loss and return loss across the simulated frequency range. Finally, in the simulation analysis of the SP8T switch, it produced 9.3 GHz of isolation bandwidth that can be used for a Gaussian pulse up to 9.3 GHz bandwidth (from 1.7 GHz to 11 GHz frequency spectrum).

Acknowledgment

The authors would like to greatly express their thanks and appreciation to the Centre for Research and Innovation Management (CRIM) and Universiti Teknikal Malaysia Melaka (UTeM) for their encouragement and help to complete this research work. This work was supported by Ministry of Higher Education (MOHE) under the research grant no: FRGS/1/2021/FKEKK/F00470.

Authors: The first five authors are from the same university and faculty, which is Universiti Teknikal Malaysia Melaka (UTeM), Jalan Hang Tuah Jaya, 76100 Durian Tunggal, Melaka, Fakulti Kejuruteraan Elektronik dan Kejuruteraan Komputer (FKEKK). Their emails are as follows:

Dr. Noor Azwan Shairi, E-mail: noorazwan@utem.edu.my;

Nursyahirah Mohd Sanusi,

E-mail: m021710008@student.utem.edu.my;

Adib Othman, E-mail: adib@utem.edu.my;

Prof. Dr. Zahriladha Zakaria, E-mail: zahriladha@utem.edu.my;

Dr. Imran Mohd Ibrahim, E-mail: imranibrahim@utem.edu.my;

Abdullah Mohammed Saghir Zobilah,

E-mail: p021710007@student.utem.edu.my;

Dr. Ariffuddin Joret, Faculty of Electrical and Electronic Engineering, Universiti Tun Hussein Onn Malaysia (UTHM), 86400, Parit Raja, Johor Malaysia, E-mail: ariff@uthm.edu.my;

REFERENCES

- [1] Kikkawa, Takamaro, Yoshihiro Masui, Akihiro Toya, Hiroyuki Ito, Takuichi Hirano, Tomoaki Maeda, Masahiro Ono et al. "CMOS Gaussian Monocycle Pulse Transceiver for Radar-Based Microwave Imaging." *IEEE Transactions on Biomedical Circuits and Systems* 14, no. 6 (2020): 1333-1345.
- [2] Feghhi, Rouhollah, Daniel Oloumi, and Karumudi Rambabu. "Tunable Subnanosecond Gaussian Pulse Radar Transmitter: Theory and Analysis." *IEEE Transactions on Microwave Theory and Techniques* 68, no. 9 (2020): 3823-3833.
- [3] Pozar, David M. *Microwave engineering*. John Wiley & Sons, 2011.
- [4] Bashri, M. S. R., Tughrul Arslan, Wei Zhou, and Nakul Haridas. "A compact RF switching system for wearable microwave imaging." In *2016 Loughborough Antennas & Propagation Conference (LAPC)*, pp. 1-4. IEEE, 2016.
- [5] Nuruliswa Abdullah, Mohamad Z. A. Abd. Aziz, Abd Shukur Jaafar. "Design of a high directive sensor for microwave imaging application." *Przeegląd Elektrotechniczny*, no. 10 (2021): 8-11
- [6] Al-Gburi, Ahmed Jamal Abdullah, Imran-Mohd Ibrahim, Zahriladha Zakaria, M. Y. Zeain, Husam Alwareth, Ayman Mohammed Ibrahim, and Hussam Hamid Kerjee. "High Gain of UWB CPW-fed Mercedes-Shaped Printed Monopole Antennas for UWB Applications." *Przeegląd Elektrotechniczny*, no. 5 (2021): 70-73
- [7] Charvat, Gregory L., Leo C. Kempel, Edward J. Rothwell, Christopher M. Coleman, and Eric L. Mokole. "A through-dielectric ultrawideband (UWB) switched-antenna-array radar imaging system." *IEEE Transactions on Antennas and Propagation* 60, no. 11 (2012): 5495-5500.
- [8] Kuwahara, Yoshihiko, and A. M. Malik. "Microwave imaging for early breast cancer detection." *New Perspect. Breast Imaging. IntechOpen* (2017): 45-71.
- [9] Brovoll, Sverre, Tor Berger, Yoann Paichard, Øyvind Aardal, Tor Sverre Lande, and Svein-Erik Hamran. "Time-lapse imaging of human heart motion with switched array UWB radar." *IEEE Transactions on Biomedical Circuits and Systems* 8, no. 5 (2014): 704-715.
- [10] Song, Hang, Shinsuke Sasada, Takayuki Kadoya, Morihito Okada, Koji Arihiro, Xia Xiao, and Takamaro Kikkawa. "Detectability of breast tumor by a hand-held impulse-radar detector: performance evaluation and pilot clinical study." *Scientific reports* 7, no. 1 (2017): 1-11.
- [11] Islam, M. T., M. Z. Mahmud, M. Tarikul Islam, S. Kibria, and M. Samsuzzaman. "A low cost and portable microwave imaging system for breast tumor detection using UWB directional antenna array." *Scientific reports* 9, no. 1 (2019): 1-13.
- [12] Ha, Byeong Wan, Chang Won Seo, Choon Sik Cho, and Young-Jin Kim. "Wideband high-isolation SPDT RF switch in 0.18-um SiGe BiCMOS technology." *Analog Integrated Circuits and Signal Processing* 87, no. 1 (2016): 11-19.
- [13] Shairi, N. A., Z. Zakaria, A. M. S. Zobilah, B. H. Ahmad, and P. W. Wong. "Design of SPDT switch with transmission line stub resonator for WiMAX and LTE in 3.5 GHz band." *ARNP J. Eng. Appl. Sci* 11, no. 5 (2016): 3198-3202.
- [14] Azhari, Afreen, Sugitani Takumi, Sogo Kenta, Takamaro Kikkawa, and Xia Xiao. "A 17 GHz bandwidth 1.2 mW CMOS switching matrix for UWB breast cancer imaging." In *2014 IEEE Biomedical Circuits and Systems Conference (BioCAS) Proceedings*, pp. 109-112. IEEE, 2014.
- [15] Chen, Lei, Liang Tian, Jin Zhou, Ai-bo Huang, and Zongsheng Lai. "A high performance PD SOI CMOS single-pole double-throw T/R switch for 2.4 GHz wireless applications." In *2009 5th International Conference on Wireless Communications, Networking and Mobile Computing*, pp. 1-4. IEEE, 2009.
- [16] Azhari, Afreen, Kuwano Yuki, Xia Xiao, and Takamaro Kikkawa. "A Tx/Rx 3-20-GHz DP16T switching matrix for breast cancer detection system." In *2016 IEEE MTT-S Latin America Microwave Conference (LAMC)*, pp. 1-4. IEEE, 2016.
- [17] Zobilah, Abdullah Mohammed Saghir, Noor Azwan Shairi, Zahriladha Zakaria, and M. S. Jawad. "RF switches in wide-, broad-, and multi-band RF front-end of wireless communications: An overview." *ARNP J. Eng. Appl. Sci* 11, no. 5 (2016): 3244-3248.
- [18] Shairi, Noor Azwan, B. H. Ahmad, and A. C. Z. Khang. "Design and analysis of broadband high isolation of discrete packaged PIN diode SPDT switch for wireless data communication." In *2011 IEEE International RF & Microwave Conference*, pp. 91-94. IEEE, 2011.
- [19] Yu, Bo, Kaixue Ma, Fanyi Meng, Kiat Seng Yeo, Parthasarathy Shyam, Shaoqiang Zhang, and Purakh Raj Verma. "Ultra-wideband low-loss switch design in high-resistivity trap-rich SOI with enhanced channel mobility." *IEEE Transactions on Microwave Theory and Techniques* 65, no. 10 (2017): 3937-3949.
- [20] Mou, Shouxian, Ma Kaixue, Yeo Kiat Seng, Bharatha Kumar Thangarasu, and Nagarajan Mahalingam. "A DC to 30GHz ultra-wideband cmos T/R switch." In *2011 Semiconductor Conference Dresden*, pp. 1-4. IEEE, 2011.
- [21] Li, Qiang, and Yue Ping Zhang. "CMOS T/R switch design: Towards ultra-wideband and higher frequency." *IEEE Journal of solid-state circuits* 42, no. 3 (2007): 563-570.
- [22] Liu, Hao-En, Xiang Lin, Hong-Yeh Chang, and Yu-Chi Wang. "10-MHz-to-70-GHz ultra-wideband low-insertion-loss SPST and SPDT switches using GaAs PIN diode MMIC process." In *2018 Asia-Pacific Microwave Conference (APMC)*, pp. 1217-1219. IEEE, 2018.
- [23] Zhu, Hao-Ran, Xin-Yu Ning, Zhi-Xiang Huang, Yong-Xin Guo, and Xian-Liang Wu. "Miniaturized, Ultra-Wideband and High Isolation Single Pole Double Throw Switch by Using π -Type Topology in GaAs pHEMT Technology." *IEEE Transactions on Circuits and Systems II: Express Briefs* 68, no. 1 (2020): 191-195.
- [24] Hadi, MH Abdul, B. H. Ahmad, Peng Wen Wong, and N. A. Shairi. "An overview of isolation improvement techniques in RF switch." *ARNP Journal of Engineering and Applied Sciences* 9, no. 3 (2014): 342-348.